Incorporating Fluorescent Nanomaterials in Organically Modified Sol-Gel Materials – Creating Single Composite Optical pH Sensors

Dávid Bartoš, Morten Rewers, Lu Wang, and Thomas Just Sørensen**

Nano-Science Center & Department of Chemistry, University of Copenhagen,

Universitetsparken 5, 2100 Copenhagen Ø, Denmark luwa@chem.ku.dk, tjs@chem.ku.dk

KEYWORDS. Nanomaterials, Single composite sol-gel, Optical pH Sensor, Ratiometric fluorescence response

Optical sensors hold the promise of providing the coupling between the tangible and the digital world that we are currently experiencing with physical sensors. The core of optical sensor development lies in materials development, where specific requirements of opposing physicochemical properties create a significant obstacle. The sensor material must provide dye retention, while ensuring porosity for analyte transport. The sensor material must provide hydrophobic pockets for dyes to ensure high signal intensity, while remaining fully hydrophobic to measure in water. We have previously reported optical sensors, where we compromised on sensor manufacturing by using a double-layer composite. Here, we report a composite organically modified sol-gel (ORMOSIL) polymer, where polystyrene (PS) nanoparticles (NPs) have been

incorporated. This allows all the opposing requirements on optical sensor materials to be fulfilled, and by introducing a hydrophobic reference dye in the fully hydrophobic compartments of the sensor material we show that we can incorporate any hydrophobic fluorophore in this material, even those which are suffering from quenching in water. In this work, PS NPs with 1,13-dimethoxyquinacridinium (DMQA) were immobilized in a composite sol-gel material with pH responsive diazaoxatriangulenium (DAOTA) dyes prior to curing. The multicomponent sensor composite was cured on a polycarbonate hemiwicking substrate, and the resulting fluorescence intensity ratiometric optical pH sensor was shown to have excellent performance. We expect that this type of composite sensor materials will allow the creation of next generation industrial chemosensors.

Introduction

The concept of optical pH sensors has been known since pH was defined by Sørensen.[1-2] Even so, disregarding colorimetric pH indicators, commercial pH sensors are mainly potentiometric pH meters that provide a linear electromotive force (EMF) response to pH obeying the Nernst equation.[2-6] There are clear advantages of optical sensors,[7-12] but complications regarding calibration: optical pH sensors report optical signals fitting to a sigmoidal curve where the response range depends on the pKa of the pH-sensitive dye,[13-14] and a limited stability of the sensor material have reduced their industrial applicability.[15-17] We have recently reported a new sensor material for optical sensors,[18] and the first high performance pH sensor using this matrix.[3] One unresolved issue with this sensor design is the reference dyes or lipophilic sensor dyes

cannot be incorporated into the matrix, without compromising performance.[19] Here, we have solved this problem, by adding an additional component to the composite sensor material.

The first generation of fiber-based optical sensors emerged around 1980.[20-21] In the following years, absorption or fluorescent-based pH indicators were incorporated in polymers, such as polystyrene,[22] polyacrylamide,[23-24] poly(methyl methacrylate) (PMMA),[25-26] and deposited on the fiber tip. Because of the high sensitivity, fluorescence sensors have been more extensively studied than other types of colorimetric sensors.[23-24, 27-28] And most of commercially available chemical optical sensors are based on fluorescence, in particular fluorescence lifetime measured in the frequency domain.[29-30, 31, 32] However, and despite the success of optical oxygen sensors,[33-36] optical chemosensors are still not prevalent on the market.[6] The challenges that remain are to improve the stability and response time of the sensor. The main problems are i) dye leakage, ii) fluorescence quenching, iii) photobleaching, and iv) slow diffusion speed of the analytes into the sensor material. There has been a strong focus on studying new matrices for sensor materials,[37-39] and on discovering improved methods for immobilizing the sensing components.[21, 40] We have described an organically modified silicon sol-gel that solves many of these issues, when it comes to creating a competitive optical pH sensor.[3, 18, 41-43] The resulting sensor material has good chemical, photochemical and thermal stability as well as fast diffusion of H^+, while excluding all other ions. The sensor material has the capacity to fully encapsulate the pH responsive dye, the ability to firmly stick to polymer and glass substrate, a long shelf-life and is fully biocompatible. In all points relating to the response of the pH sensor response the behavior this material is close to ideal. However, the newly designed sensor, based on a ratiometric response in fluorescence intensity, has an issue incorporating – typically lipophilic – reference dye in this highly hydrophilic sensor material.

In the ideal sensor, the reference dye – a photostable fluorescent dye that is inert to pH – must be an integral part of the sensor material. The role of the reference dye is to compensate for changes in the optical system, analogues in concept to the reference electrode of a conventional pH meter. Quantum dots (QDs) have been used as reference dyes due to good light stability and high quantum yield,[44-46] but as there remains issues with biocompatibility we prefer molecular fluorophores. We have reported optical pH sensors with an intensity ratiometric response, where different dyes have been incorporated as part of the sensor material.[42] All the reference dyes shown in figure 1 suffer from unspecific quenching of the reference dye by water,[47] even when the highly photostable terrylene based dye (TDI) is incorporated in the most hydrophobic of the ORMOSIL matrices.[19, 48] The current solution is to make an optode where the reference dye is kept in a dry environment, by depositing it in polystyrene on the back of the substrate.[3] This optode configuration is not ideal for industrial production, and the temperature stability of polystyrene limits the application areas of the resulting optical pH sensor.

Here, we present a new composite sensor material to alleviate the issues we have seen with the reference dye. We suggest to incorporate the reference dye in polystyrene nanoparticles into the ORMOSIL prior to curing, thereby creating hydrophobic polystyrene compartments in the ORMOSIL network. This design segregates the reference dye from the water contacting material and we obtain a constant fluorescence signal from the reference dye. The design simplifies production as the optode – the active element in the optical sensor – is created by deposition of a solution directly on the substrate. The design concept is illustrated in **Figure 1**. A concern is the distribution of nanoparticles is not homogeneous, but as we probe an area measured in millimeters, we aim to prove that any variation in the stochastic distribution of the nanoparticles

in the sol-gel will be vanishing, and that an average fluorescence intensity per volume will be observed.[49]

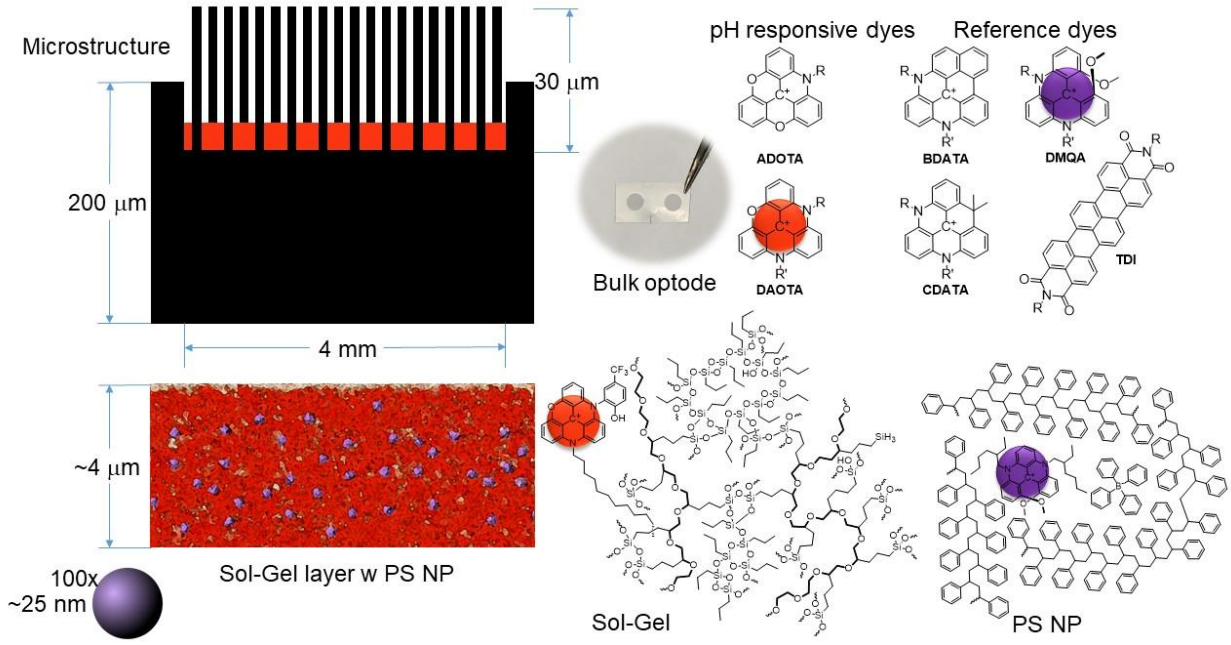

Figure 1. Representation of the elements in the composite materials used in an optical pH sensor illustrating the scale of the different elements. Left, polycarbonate substrate and microstructure with sensor material shown to scale, with the sol-gel layer magnified to show the relative scale of the polystyrene nanoparticles. Right, pH responsive azadioxatriangulenium (ADOTA) and diazaoxatriangulenium (DAOTA) dyes,[50-51] and lipofilic reference benzo- and carbon-bridged diazatriangulenium (BDATA and CDATA),[52-53] terrylenediimide (TDI),[54] and 1,13-dimethoxyquinacridinium (DMQA) dyes.[55] The local environment of pH responsive and reference dyes in sol-gel and polystyrene nanoparticle is illustrated.

Optical pH sensors based on nano/microparticles in the gel matrix have been reported previously. The dyes were encapsulated with plasticizers or surfactants and form lipophilic particles, then they were embedded in hydrogels and polymers such as polyvinyl alcohol (PVA),[56] polyacrylamide,[57] and agarose.[58] The main difference to our work reported here, is that they

mainly focus on hydrogel-based sensor materials that are not stable in industrial applications. The approach based on organically modified silicate materials are more robust,[18] and we hope to be able to use the sensor material reported here to incorporate not only molecular dyes, but also more complex fluorescent materials.[49, 59-61]

Methods and Materials

Reagents. 4-(2-hydroxyethyl)-1-piperazineethanesulfonic acid (HEPES), sodium hydroxide (NaOH), hydrochloric acid (HCl), toluene, dichloromethane (CH_2Cl_2), ethanol, sodium dodecyl sulfate (SDS), 3-(Glycidoxy)propyltrimethoxysilane (GPTMS; >98%), and polystyrene (PS; Lot.: 07430MO-404), borontrifluoride diethyletherate ($BF_3O(CH_2CH_3)_2$) were obtained from Sigma-Aldrich. Propyl triethoxysilane (PrTES; 97%) was purchased from Alfa Aesar. The pH-responsive dye N-(2-hydroxy-5-(trifluoromethyl)phenyl)-N'-(dodecyl)-diazaoxatriangulenium hexafluorophosphate, DAOTA) and the reference dye *N,N'*-(2-ethylhexyl)-1,13-dimethoxyquinacridinium hexafluorophosphate (DMQA) were synthesized as previously reported.[62-63] Polycarbonate substrate (4 mmØ)[48] was obtained from NIL Technology, Denmark. All salts and solvents used were analytical grade or higher. All testing solutions were prepared by dissolving appropriate salts into deionized water (Milli-Q).

Instrumentation and measurements. Emulsification was done with the sonicator (XS-sonic, FS-680N). Centrifugation was done by the centrifuge (MiniSpin® plus, Eppendorf) with disposable Eppendorf tubes (1.5 ml). The fluorescence spectra for the DMQA-doped NP were recorded using a Cary Eclipse fluorescence spectrophotometer (Agilent Technologies). Scanning electron microscopic (SEM) images were obtained under Jeol 7800F-prime Scanning electron microscope (10 kV). Images and fluorescence spectra of one spot were obtained by a wide-fields

microscope (ZEISS, filter: 475/40ex, 510+em). Fluorescence intensity distribution of the sensor spots were also evaluated by the Microplate Reader (BMG LABTECH, PHERAstar *FSX*) with sensor spots glued on the GREINER 96 F-BOTTOM microplate (filter, FP 540-20/590-20 for DAOTA and HTRF 337/665-620 for DMQA; matrix scan 20×20, 4 mmØ).

A home-built hardware platform containing an LED light source and spectrometer was used to measure the fluorescence response of the pH optical sensor.[48] The spectrometer acquired spectra with background light subtraction for each measurement.

Preparation of the optode

Preparation of the reference dye-doped PS nanoparticles. 19.24 mg of PS was dissolved in 2 ml of toluene/CH_2Cl_2 (v/v, 4:1). 2.4 mg of the reference dye (DMQA) was dissolved herein. 14 mg of SDS was dissolved in 14 ml of Milli-Q water by stirring for 30 min at room temperature. The two solutions were mixed and the two-phase system was sonicated with the probe (7 mmØ, sonicating power: 70 W) with 1 second on and 1 second off timing for a total duration of 60 seconds while stirring at 300 rpm. This process was repeated 5 times with a waiting time of 60 minutes between each sonication during which the vile is left stirring at 300 rpm with a closed cap. After the fifth sonication, the sample is left with an open cap on and stirring at 300 rpm for 48 hours to evaporate all the toluene. The obtained milky solution was centrifuged (13 000 rpm, 5 min), washed with ethanol/water (v/v, 1:3), and then centrifugation. The obtained centrifugate was dried in the oven at 35 ℃.

The sol-gel matrix. The material was prepared as previously reported.[48] Briefly,

a) Procedure for preparation of PrTES-gel component: 1.25 ml PrTES was dissolved in 2 ml

absolute ethanol while stirring. Thereafter, 0.4 ml of 0.1 M HCl solution was added dropwise. This mixture was left stirring for 7 days.

b) Procedure for preparation of GPTMS-gel component: 2.4 mg pH-responsive dye was dissolved in 5.5 ml of absolute ethanol. 3 ml of GPTMS (27 mmol) was added while stirring. Then 0.4 ml of cold $BF_3O(CH_2CH_3)_2$ was added dropwise. The mixture was stirred for 30 min then 1 ml of Milli-Q water was added to the solution. The resulting mixture was stirred for 4 h.

c) Combination of the two sol-gels: When the two gel components have been prepared they were combined in (PrTES:GPTMS) volume ratio of 3:7 and left agitated for one day.

d) Combination of the PS particles with the sol-gel: 6 mg of the reference dye-doped PS nanoparticles were added into 0.5 ml of aged sol-gel. The resulting sol-gel was sonicated in an ultrasonic bath for 1 minute to properly disperse the nanoparticles.

Deposition and curing of sensor material on a polycarbonate microstructure spot. 2 μl of sol-gel material was deposited on a microstructured polycarbonate spot. With a piece of flat polycarbonate, the excess sensor material from the deposition was spread across the sensor spot to remove excess gel and produce an even thickness. The residual sol-gel was removed with the extra piece of flat polycarbonate. The resulting sensor spots were left for 30 minutes, allowing the ethanol to evaporate, before they were placed in the oven (110°C, 3 h) for curing. The sensor spots were immersed in HEPES buffer (20 mM, pH 7.6) for 1 h and rinsed with Milli-Q water before use.

Results and discussion

Sensor material synthesis

The reference dye *N,N'*-(2-ethylhexyl)-1,13-dimethoxyquinacridinium (DMQA),[55, 64-66] see **Figure S1**, belongs to the class of highly photostable triangulenium fluorophores (λ_{em} = 660nm).[50-51, 67] The dye has no response to pH, but it suffers from fluorescence quenching when exposed to water.[65] Furthermore, we have observed that, in the ORMOSIL sol-gel sensor material, DMQA is not chemically stable.[42] To avoid quenching and increase the chemical stability DMQA-doped polystyrene nanoparticles were synthesized by the reproducible and scalable emulsification method developed in-house.[68] Briefly, sodium dodecyl sulfate (SDS) was used as a stabilizing agent for the DMQA/polystyrene/toluene droplets formed upon emulsification of a water/toluene mixture. The toluene was removed from the system by slow evaporation over 48 h with continued stirring. The extra surfactant was then removed by washing with ethanol/water (v/v, 1:3) and the purified DMQA-doped PS NPs were obtained after the evaporation of the remaining solvent. **Figure 2** shows the fluorescence excitation and emission spectra, the size distribution and selected SEM images of the DMQA-doped PS NPs.

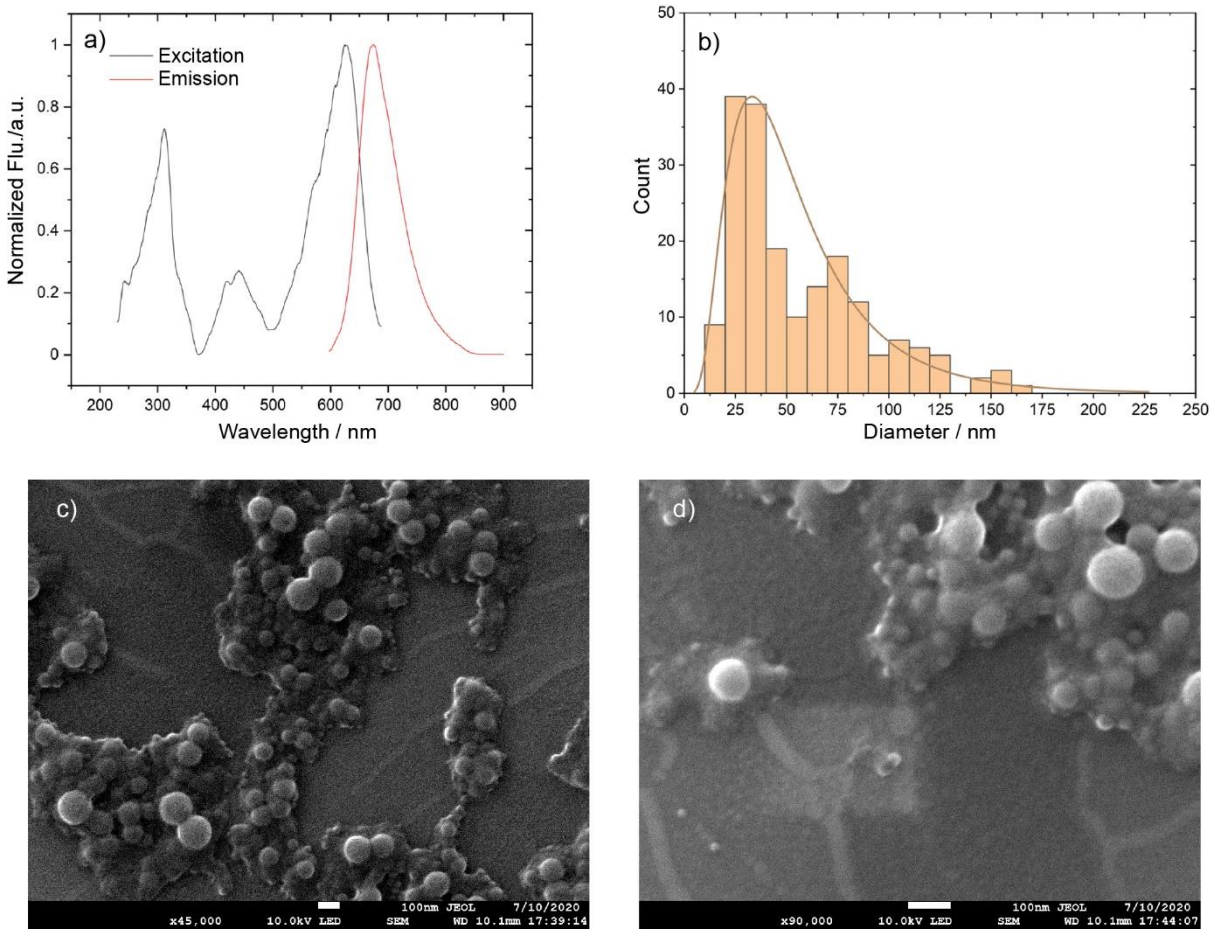

Figure 2. a) Normalized excitation and emission spectra for the DMQA NPs in water. b) PS NP size distribution (n=187, bin size: 10 nm) was counted from the SEM image c). cd) SEM images for this PS NP sample (scale bars: 100 nm).

The triangulenium based pH-sensitive DAOTA dyes,[13, 69] and the sol-gel synthesis of the sensor material is reported in our previous work.[3, 18, 43] Previous work reports on sensors with dyes that have a triethoxysilane group in their structure, which covalently bind the dye to the silicate network of the ORMOSIL. Here, we use a pH-responsive DAOTA dye (**Figure S1**) that physisorbs in the ORMOSIL material. The performance of the physisorption approach is similar to that of the chemisorpion for these dyes.[19] To make the new sensor material, an aliquot of DMQA-doped PS NPs were mixed with matured sol-gel containing DAOTA. This mixture was

then deposited onto a 4 mmØ micro-structured polycarbonate substrate.[70] After curing (110°C, 3 h) and conditioning in HEPES buffer (20 mM, 1 h), the new pH sensor spot was ready to use. The details of the full procedure can be found in the experimental section.

More than ten optodes were made. First, we investigated the structure of the resulting sensor material on the micro- and nanoscales. Then, we evaluate the distribution of the DMQA-doped PS NPs to ensure that the nanoparticles provide a uniform signal across the 4 mmØ spot. And finally we investigated the performance of the resulting optical pH sensor.[4]

Structure of new sensor material

First, a visual inspection was performed to see if the homogeneous intensity could be observed across the 4 mmØ spots using an epifluorescence wide-field microscope equipped with filter sets matching the DAOTA and DMQA emissions. Images of a single sensor spot are shown under different magnifications in **Figure 3ab**. The images capture emission signals from both the DMQA inside the PS NPs and the DAOTA embedded in the sol-gel. The red color shows the fluorescence intensity of both dyes and we see that the intensity is distributed evenly across the microstructure.

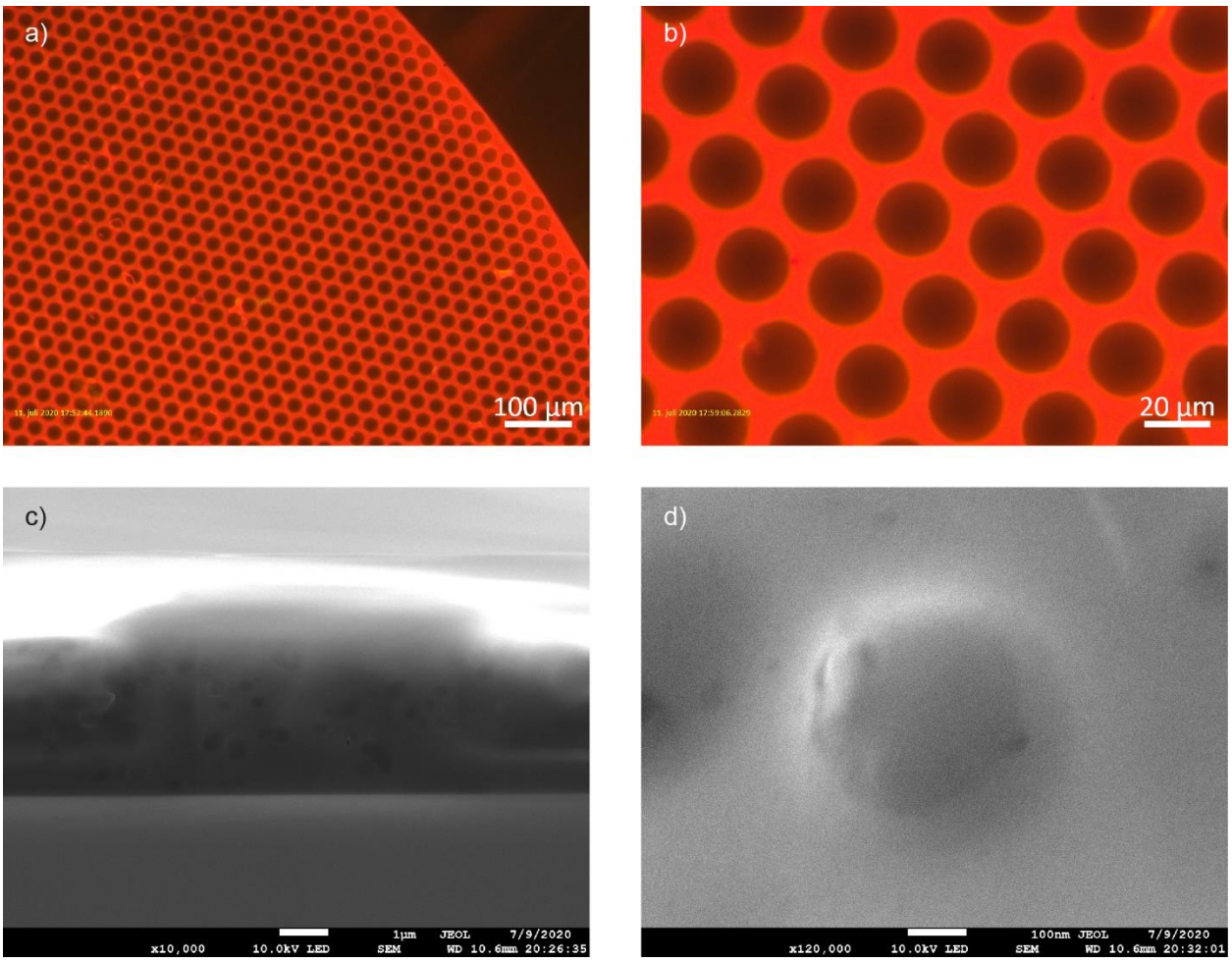

Figure 3. Images of a pH-responsive optical sensor spot observed under the microscope with magnifications of a) 10x and b) 50x. Cross-section SEM images of pH-responsive sol-gel with DMQA encapsulated PS NPs spin-coated and cured on Si-wafer. Scale bar: c) 1µm and d) 100 nm.

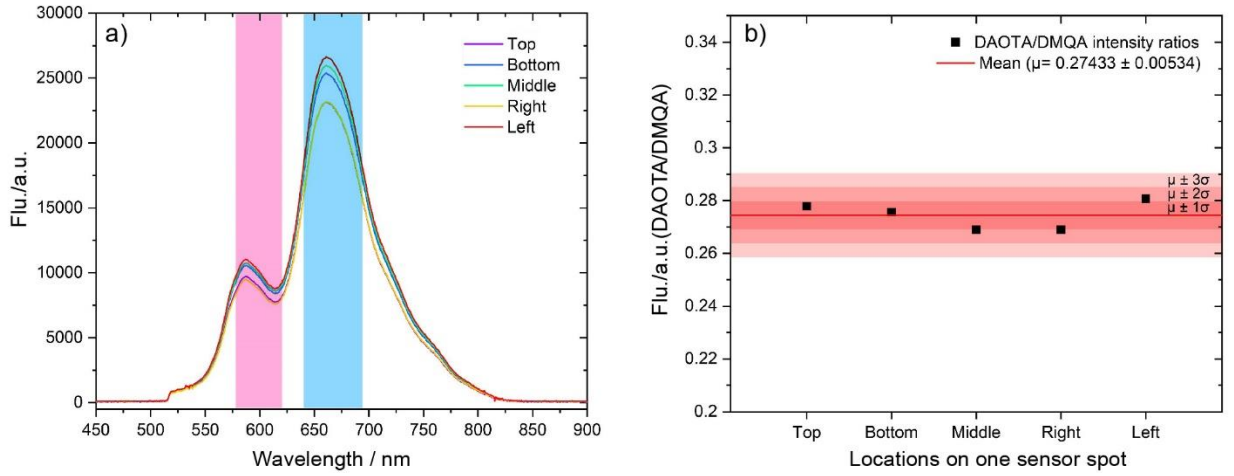

Figure 4. a) Fluorescence emission spectra of one pH-responsive sensor spot loaded with DMQA doped PS NPs at five different locations (DAOTA, 580-620 nm, pink band; DMQA, 640-695 nm, blue band). b) Ratios of integrated areas for DAOTA and DMQA with calculated mean μ and standard deviation σ.

To further probe the structure of the sensor material, SEM images were recorded. **Figure 3cd** show the clear spherical edge of the NPs, which proves that the NPs do not dissolve in the sol-gel and remain intact in the curing process. As expected, the nanoparticles do not disperse evenly in the sensor gel on the nanoscale (**Figure 3c**). But as all applications measure on the macroscopic scale, where the integrated optical signal is recovered from a mm^2 area rather than from individual point on the nanoscale, we do not expect this to be an issue. For instance, the optical fiber on our hardware probes an area exceeding 1 mmØ. To prove this point, two experiments were performed. First, five different locations on a single optical sensor spot were measured to evaluate the uniformity of the sensor with 20x magnification (**Figure 4**, see illustration in **Figure S2**). To produce the readout from the sensor spot, each spectrum was integrated from 580 to 620 nm for DAOTA and 640 to 695 nm for DMQA, and the ratios of integrated intensities of these two peak areas were plotted in **Figure 4b** corresponding to the positions of the data acquisition (top, bottom, middle, right or left on the spot). The small

deviation indicates the sensor material has a uniform NP distribution. To quantify this result, we investigated ten sensor spots in a fluorescence plate reader. In this experiment, 100 points across each sensor spot were investigated, and we found that the variation in DAOTA/DMQA fluorescence intensity ratio was lower than 5 % (**Table 1**, see data treatment progress in **Figure S3**), fully consistent with the 2 % estimated from the microscopy measurements. We thus conclude that the fluorescence signal is homogeneous on the scale of millimeters, therefore not impacting the area probed by the optical fiber.

Table 1. Average values, standard deviations and variations for the DAOTA/DMQA fluorescence intensity of 10 sensor spots measured by the fluorescence plate-reader

Sensor spot	**1**	**2**	**3**	**4**	**5**	**6**	**7**	**8**	**9**	**10**
Average Sensor signal of 100 points	**1.48**	**1.66**	**1.27**	**0.65**	**0.59**	**0.91**	**1.60**	**1.12**	**0.99**	**0.94**
Standard deviation	**0.07**	**0.04**	**0.03**	**0.03**	**0.03**	**0.04**	**0.04**	**0.04**	**0.02**	**0.02**
Variation	**5%**	**2%**	**3%**	**5%**	**5%**	**4%**	**3%**	**4%**	**2%**	**2%**

Performance of new optical sensor

pH response was tested in HEPES buffer solution (20 mM) by the home-built fluorescence miscroscope set-up (**Figure S4**).[48] **Figure 5** shows the fluorescence emission spectra at different pH adjusted by pumping HCl (1 M) or NaOH (1 M). Each spectrum is the mean value of 3 spectra obtained after fluorescence intensity reached equilibrium for every pH adjustment (**Figure 5**). Both of the emission bands (DAOTA, 595 nm; DMQA, 660 nm) decrease with the decreasing of pH value. However, the decrease of the band at 660 nm is due to the overlap with

the peak 595nm, as it has been confirmed DMQA has no fluorescence response to pH when it is in the gel phase.[41] The normalized and smoothed fluorescence spectra were shown in **Figure S5**, and the pH is evaluated by the ratiometric signal of the integrated peak areas (DAOTA/DMQA).

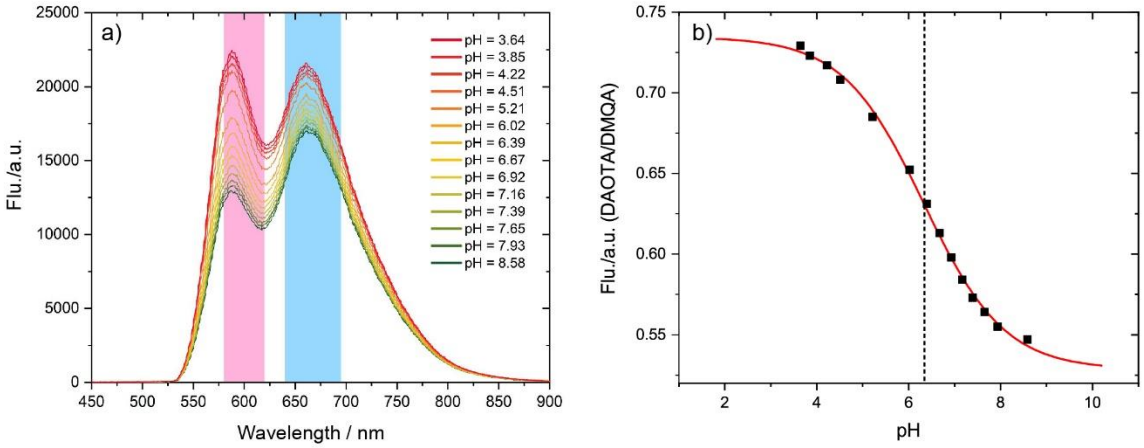

Figure 5. a) Fluorescence spectra of the pH optode at different pH with integration ranges for pH-responsive dye (DAOTA, 580-620 nm, pink band) and the reference dye (DMQA, 640-695 nm, blue band). b) The calibration curve of the optical pH sensor.

By monitoring the sensors response to pH, we could see the responses are reversible and repeatable (**Figure S6**). **Figure 5b** shows the sigmoidal calibration curve fitted to the pH response data from **Figure 5a**. pKa of this pH-responsive dye is 6.33 ± 0.05 consistent with the pKa value 6.5 from previous reports based on the same dye.[62] This indicated the sensor material with and without nanoparticles have similar photophysical properties. The slight difference of pKa values observed between here and our reported studies[48, 71] may just as well be due to the structural difference between physisorped and chemisorbed dyes.

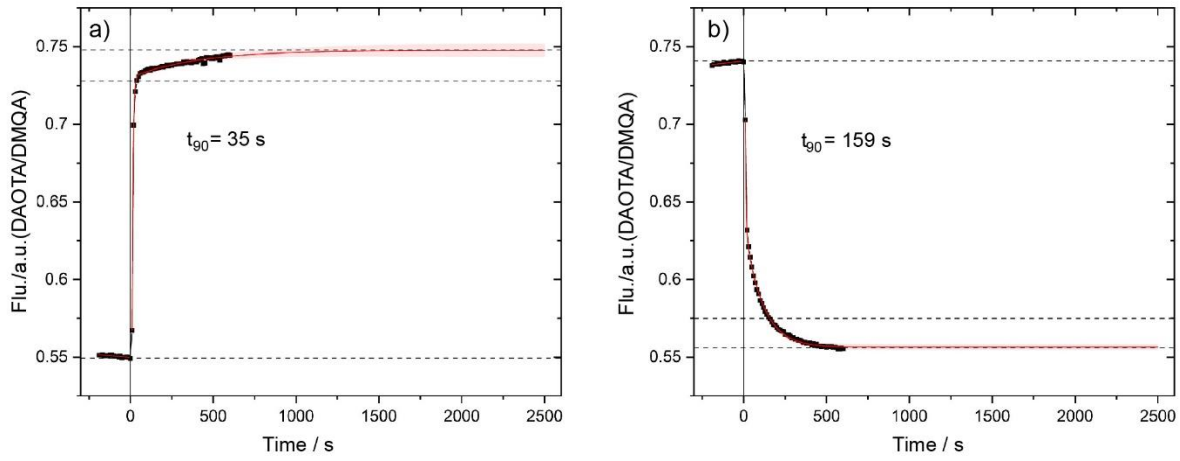

Figure 6: Time response of the optical sensor spot with pH change from a) 9.09 to 3.71 and b) 3.72 to 9.09 (data was captured every 10 s).

The response time of a pH sensor depends on the rate of diffusion of proton.[4, 43] The main factors governing these rates are the nature of the sol-gel and the thickness of the sol-gel layer. For a specific sensor, response time is also related to the measurement procedure such as the direction and the range of the pH change. Response time here was calculated based on two exponential decay functions.[48] **Figure 6** shows t_{90} is 35 s for the pH change from 9.09 to 3.71 and 150 s for 3.72 to 9.09. The response is slower for the change from acid to base because the sol-gel selectively allows for proton transport.[18] In our previous report, t_{90} of such sol-gel based optical pH sensor is 19s for the pH change from 8 to 3, and 51s for 3 to 8. We hypothesize that the cause of the slower response here is that the proton transporting PEG-like networks are impeded by the PS NPs or some aggregated NPs in the sol-gel.

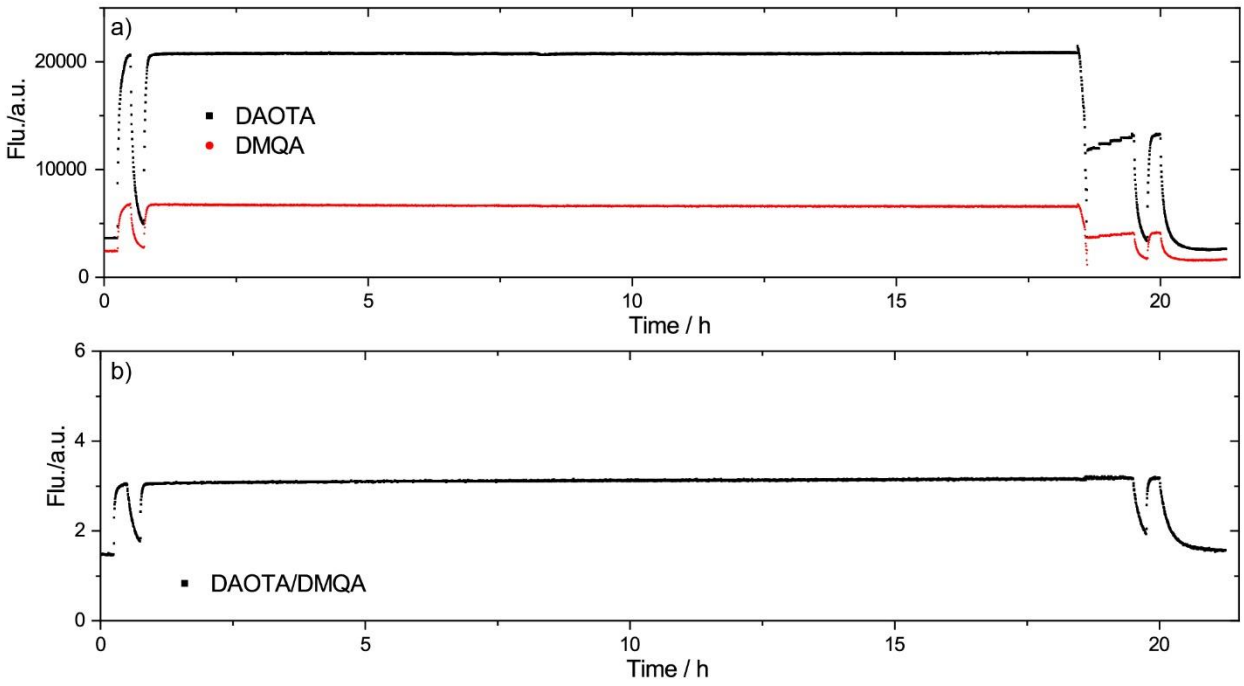

Figure 7. Stability testing for one pH optical sensor spot. The integrated fluorescence intensity for a) both dyes and b) their ratio plotted versus time (data was captured every 18 s).

Stability was tested by a long-term continually fluorescence intensity measurement which lasted 21 hours in HEPES (20 mM, r.t. and in the dark). pH response was tested before and after the long-term measurement. **Figure 7a** shows the integrated values for both dyes were stable during the long-term measurement, and so was the ratio signal of the two dyes (**Figure 7b**). The drift of the sensor signal is calculated to be $1.55 \cdot 10^{-3}$ /h. The positive drift due to the degradation of DMQA exceeds that of the pH responsive dye.[72]

The trace in Figure 7 shows a kink at 18.5 h, where the level of buffer solution due to evaporation dropped below the fiber tip. From this point, interface reflection weakened the fluorescence signal. Figure 7a shows that both DAOTA and DMQA signals changed significantly, but Figure 7b shows that the sensor signal did not vary although an increase in the noise is evident.

Overall this proof-of-concept optical pH sensor exhibits acceptable response time and shows active range at pH 6.33±1.5. High stability, reproducible sensor spots indicates that this novel composite material is a promising candidate for developing optical sensors for industrial applications.

CONCLUSION

After ten years of research, we were able to present in this paper a sensor material for optical chemosensors that has hydrophilic areas that allow for fast analyte transport and hydrophobic areas able to host water sensitive dyes. By doping the hydrophobic dyes into the polystyrene nanoparticles that can be produced reproducibly and in bulk, we successfully prepared an optical pH sensor where the reference dye is protected from water-quenching . The work reported here shows that we are able to produce optical chemosensors in a single deposition. We have developed a composite sensor material that is both hydrophilic and hydrophobic, and that maintains all the beneficial properties of the parent ORMOSIL composite.

SEM images proved that the polystyrene nanoparticles are incorporated intact into the sensor material, and we were able to prove that the nanoparticles are evenly distributed in the sensor material. We prepared pH optodes using the new sensor materials, and proved that we can move from separated, two-layer optode,[3] to a single layer optode where both reference and pH responsive dyes is integrated into the sensor material, while maintaining the properties of the original optical pH sensor.

Several pH sensors were prepared. They showed no obvious dye leakage, were found to maintain a fast and reliable response, and we found that the pH optical sensor was stable for more than

5000 measurements. The next step will be to build a dedicated hardware, and incorporate the new sensor material in an industrial sensor.

ASSOCIATED CONTENT

Supporting Information.

Supporting Information includes structures of the dyes, illustrations of measurement setups and pH response data.

AUTHOR INFORMATION

Corresponding Authors

* Email: tjs@chem.ku.dk

* Email: luwa@chem.ku.dk

Author Contributions

The manuscript was written through contributions of all authors. All authors have given approval to the final version of the manuscript.

Notes

TJS is the founder of FRS-systems ApS, a spin-out company from the University of Copenhagen commercializing optical sensors.

ACKNOWLEDGMENT

The authors thank Novo Nordisk Fonden (grant #NNF19OC0057136), Villum Fondet (grant#14922), Carlsbergfondet and the University of Copenhagen for support. Laura Grenier is thanked for her input to the final manuscript.

REFERENCES

1. Sørensen, S. P. L., Über die Messung und die Bedeutung der Wasserstoffionenkonzentration bei enzymatischen Prozessen. *Biochem. Zeitschr.* **1909,** *21*, 131-304.
2. Steinegger, A.; Wolfbeis, O. S.; Borisov, S. M., Optical Sensing and Imaging of pH Values: Spectroscopies, Materials, and Applications. *Chem. Rev.* **2020**.
3. Frankær, C. G.; Hussain, K. J.; Dorge, T. C.; Sorensen, T. J., Optical Chemical Sensor Using Intensity Ratiometric Fluorescence Signals for Fast and Reliable pH Determination. *ACS Sens* **2019,** *4* (1), 26-31.
4. Frankær, C. G.; Sørensen, T. J., A Unified Approach for Investigating Chemosensor Properties – Dynamic Characteristics. *Analyst* **2019,** *submitted*.
5. Borisov, S. M.; Wolfbeis, O. S., Optical biosensors. *Chem. Rev.* **2008,** *108* (2), 423-461.
6. Wolfbeis, O. S., Probes, sensors, and labels: why is real progress slow? *Angew Chem Int Ed Engl* **2013,** *52* (38), 9864-5.
7. Card, C.; Clark, K.; Furey, J., Adoption of Single-Use Sensors for BioProcess Operations. *BioProcess International* **2011,** *9* (5), 36–42.
8. Weichert, H.; Lüders, J.; Becker, M.; Adams, T.; Weyand, J., Integrated Optical Single-Use Sensors: Moving Toward a True Single-Use Factory for Biologics and Vaccine Production. *BioProcess International* **2014,** *12* (Supp. 5), 20–24.
9. Janzen, N. H.; Schmidt, M.; Krause, C.; Weuster-Botz, D., Evaluation of fluorimetric pH sensors for bioprocess monitoring at low pH. *Bioproc Biosyst Eng* **2015,** *38* (9), 1685–1692.
10. Wencel, D.; Abel, T.; McDonagh, C., Optical chemical pH sensors. *Anal. Chem.* **2014,** *86* (1), 15–29.
11. Newton, J.; Oeggl, R.; Janzen, N. H.; Abad, S.; Reinisch, D., Process adapted calibration improves fluorometric pH sensor precision in sophisticated fermentation processes. *Engineering in Life Sciences* **2020**.
12. Wu, D.; Sedgwick, A. C.; Gunnlaugsson, T.; Akkaya, E. U.; Yoon, J.; James, T. D., Fluorescent chemosensors: the past, present and future. *Chem. Soc. Rev.* **2017,** *46* (23), 7105-7123.
13. Frankær, C. G.; Rosenberg, M.; Santella, M.; Hussain, K. J.; Laursen, B. W.; Sørensen, T. J., Tuning the pKa of a pH Responsive Fluorophore and the Consequences for Calibration of Optical Sensors Based on a Single Fluorophore but Multiple Receptors. *ACS Sensors* **2019,** *4* (3), 764-773.
14. Dillingham, P. W.; Alsaedi, B. S. O.; Granados-Focil, S.; Radu, A.; McGraw, C. M., Establishing Meaningful Limits of Detection for Ion-Selective Electrodes and Other Nonlinear Sensors. *ACS Sensors* **2020,** *5* (1), 250-257.
15. Dalfen, I.; Dmitriev, R. I.; Holst, G.; Klimant, I.; Borisov, S. M., Background-free fluorescence decay time sensing and imaging of pH with highly photostable diazaoxotriangulenium dyes. *Anal. Chem.* **2018**.

16. Weidgans, B. M.; Krause, C.; Klimant, I.; Wolfbeis, O. S., Fluorescent pH sensors with negligible sensitivity to ionic strength. *Analyst* **2004,** *129* (7), 645-650.
17. Mosshammer, M.; Strobl, M.; Kuhl, M.; Klimant, I.; Borisov, S. M.; Koren, K., Design and Application of an Optical Sensor for Simultaneous Imaging of pH and Dissolved O-2 with Low Cross-Talk. *Acs Sensors* **2016,** *1* (6), 681-687.
18. Frankær, C. G.; Hussain, K. J.; Rosenberg, M.; Jensen, A.; Laursen, B. W.; Sørensen, T. J., Biocompatible microporous organically modified silicate material with rapid internal diffusion of protons. *Acs Sensors* **2018,** *3* (3), 692-699.
19. Sørensen, T. J.; Rosenberg, M.; Laursen, B. W. Patent WO/2015/058778, Sol-Gel Based Matrix. 2015.
20. Norris, J. O. W., Current Status and Prospects for the Use of Optical Fibers in Chemical-Analysis - a Review. *Analyst* **1989,** *114* (11), 1359-1372.
21. Lin, J., Recent development and applications of optical and fiber-optic pH sensors. *TrAC Trends in Analytical Chemistry* **2000,** *19* (9), 541-552.
22. Kirkbright, G. F.; Narayanaswamy, R.; Welti, N. A., Fibre-Optic Ph Probe Based on the Use of an Immobilized Colorimetric Indicator. *Analyst* **1984,** *109* (8), 1025-1028.
23. Tan, W.; Shi, Z.; Smith, S.; Birnbaum, D.; Kopelman, R., Submicrometer Intracellular Chemical Optical Fiber Sensors. *Science* **1992,** *258* (5083), 778-781.
24. Tan, W.; Shi, Z.; Kopelman, R., Development of Submicron Chemical Fiber Optic Sensors. *Analytical Chemistry* **1992,** *64* (23), 2985-2990.
25. Egami, C.; Takeda, K.; Isai, M.; Ogita, M., Evanescent-wave spectroscopic fiber optic pH sensor. *Opt Commun* **1996,** *122* (4-6), 122-126.
26. Egami, C.; Suzuki, Y.; Sugihara, O.; Fujimura, H.; Okamoto, N., Wide range pH fiber sensor with congo-red-and methyl-red-doped poly (methyl methacrylate) cladding. *Japanese journal of applied physics* **1997,** *36* (5R), 2902.
27. Schäferling, M., The Art of Fluorescence Imaging with Chemical Sensors. *Angewandte Chemie International Edition* **2012,** *51* (15), 3532-3554.
28. Ueno, T.; Nagano, T., Fluorescent probes for sensing and imaging. *Nature methods* **2011,** *8* (8), 642-645.
29. Christiansen, M. P.; Klaff, L. J.; Bailey, T. S.; Brazg, R.; Carlson, G.; Tweden, K. S., A prospective multicenter evaluation of the accuracy and safety of an implanted continuous glucose sensor: the PRECISION study. *Diabetes technology & therapeutics* **2019,** *21* (5), 231-237.
30. Shih, W. M.; Gryczynski, Z.; Lakowicz, J. R.; Spudich, J. A., A FRET-based sensor reveals large ATP hydrolysis-induced conformational changes and three distinct states of the molecular motor myosin. *Cell* **2000,** *102* (5), 683-694.
31. PyroScience Sensor Tehcnology, https://www.pyroscience.com/en/ 11/11/2020 9:25
32. PreSens precision sensing, https://www.presens.de/products/ph, 11/11/2020 9:25
33. Wang, X. D.; Wolfbeis, O. S., Optical methods for sensing and imaging oxygen: materials, spectroscopies and applications. *Chem Soc Rev* **2014,** *43* (10), 3666-761.
34. Wolfbeis, O. S., Luminescent sensing and imaging of oxygen: Fierce competition to the Clark electrode. *Bioessays* **2015,** *37* (8), 921-928.
35. Wolfbeis, O. S., Materials for fluorescence-based optical chemical sensors. *J. Mater. Chem.* **2005,** *15* (27-28), 2657-2669.
36. McDonagh, C.; Burke, C. S.; MacCraith, B. D., Optical chemical sensors. *Chem. Rev.* **2008,** *108* (2), 400-422.

37. Jerónimo, P. C.; Araújo, A. N.; Montenegro, M. C. B., Optical sensors and biosensors based on sol–gel films. *Talanta* **2007,** *72* (1), 13-27.
38. Wang, E.; Chow, K.-F.; Kwan, V.; Chin, T.; Wong, C.; Bocarsly, A., Fast and long term optical sensors for pH based on sol–gels. *Analytica chimica acta* **2003,** *495* (1-2), 45-50.
39. Lee, S. T.; Gin, J.; Nampoori, V.; Vallabhan, C.; Unnikrishnan, N.; Radhakrishnan, P., A sensitive fibre optic pH sensor using multiple sol-gel coatings. *Journal of Optics A: Pure and Applied Optics* **2001,** *3* (5), 355.
40. Wencel, D.; Abel, T.; McDonagh, C., Optical chemical pH sensors. *Analytical chemistry* **2014,** *86* (1), 15-29.
41. Rosenberg, M.; Laursen, B. W.; Frankær, C. G.; Sørensen, T. J., A Fluorescence Intensity Ratiometric Fiber Optics–Based Chemical Sensor for Monitoring pH. *Advanced Materials Technologies* **2018,** *3* (12), 1800205.
42. Sørensen, T. J.; Rosenberg, M.; Frankær, C. G.; Laursen, B. W., An Optical pH Sensor Based on Diazaoxatriangulenium and Isopropyl‐Bridged Diazatriangulenium Covalently Bound in a Composite Sol‐Gel. *Advanced Materials Technologies* **2018,** *0* (0), 1800561.
43. Frankær, C. G.; Sørensen, T. J., Investigating the Time Response of an Optical pH Sensor Based on a Polysiloxane–Polyethylene Glycol Composite Material Impregnated with a pH-Responsive Triangulenium Dye. *ACS Omega* **2019,** *4* (5), 8381-8389.
44. Jiang, Z.; Yu, X.; Hao, Y., Design and fabrication of a ratiometric planar optode for simultaneous imaging of pH and oxygen. *Sensors-Basel* **2017,** *17* (6), 1316.
45. Wang, X.; Boschetti, C.; Ruedas-Rama, M. J.; Tunnacliffe, A.; Hall, E. A., Ratiometric pH-dot ANSors. *Analyst* **2010,** *135* (7), 1585-1591.
46. Wang, X. d.; Chen, X.; Xie, Z. x.; Wang, X. r., Reversible optical sensor strip for oxygen. *Angewandte Chemie* **2008,** *120* (39), 7560-7563.
47. Dobretsov, G.; Syrejschikova, T.; Smolina, N., On mechanisms of fluorescence quenching by water. *Biophysics* **2014,** *59* (2), 183-188.
48. Frankær, C. G.; Hussain, K. J.; Dorge, T. C.; Sørensen, T. J., Optical chemical sensor using intensity ratiometric fluorescence signals for fast and reliable pH determination. *Acs Sensors* **2018,** *4* (1), 26-31.
49. Benson, C. R.; Kacenauskaite, L.; VanDenburgh, K. L.; Zhao, W.; Qiao, B.; Sadhukhan, T.; Pink, M.; Chen, J.; Borgi, S.; Chen, C.-H.; Davis, B. J.; Simon, Y. C.; Raghavachari, K.; Laursen, B. W.; Flood, A. H., Plug-and-Play Optical Materials from Fluorescent Dyes and Macrocycles. *Chem* **2020,** *6* (8), 1978-1997.
50. Laursen, B. W.; Krebs, F. C., Synthesis of a triazatriangulenium salt. *Angew. Chem. Int. Ed.* **2000,** *39* (19), 3432-3434.
51. Laursen, B. W.; Krebs, F. C., Synthesis, structure, and properties of azatriangulenium salts. *Chem. Eur. J.* **2001,** *7* (8), 1773-1783.
52. Rosenberg, M.; Rostgaard, K. R.; Liao, Z.; Madsen, A. Ø.; Martinez, K. L.; Vosch, T.; Laursen, B. W., Design, synthesis, and time-gated cell imaging of carbon-bridged triangulenium dyes with long fluorescence lifetime and red emission. *Chemical Science* **2018,** *9* (12), 3122-3130.
53. Rosenberg, M.; Santella, M.; Bogh, S. A.; Muñoz, A. V.; Andersen, H. O. B.; Hammerich, O.; Bora, I.; Lincke, K.; Laursen, B. W., Extended Triangulenium Ions: Syntheses and Characterization of Benzo-Bridged Dioxa- and Diazatriangulenium Dyes. *The Journal of Organic Chemistry* **2019,** *84* (5), 2556-2567.

54. Holtrup, F. O.; R. J. Müller, G.; Quante, H.; De Feyter, S.; De Schryver, F. C.; Müllen, K., Terrylenimides: New NIR Fluorescent Dyes. *Chemistry – A European Journal* **1997,** *3* (2), 219-225.
55. Herse, C.; Bas, D.; Krebs, F. C.; Burgi, T.; Weber, J.; Wesolowski, T.; Laursen, B. W.; Lacour, J., A highly configurationally stable [4]heterohelicenium cation. *Angew. Chem. Int. Ed.* **2003,** *42* (27), 3162-3166.
56. Kim, M. D.; Dergunov, S. A.; Lindner, E.; Pinkhassik, E., Dye-Loaded Porous Nanocapsules Immobilized in a Permeable Polyvinyl Alcohol Matrix: A Versatile Optical Sensor Platform. *Analytical Chemistry* **2012,** *84* (6), 2695-2701.
57. Krause, C.; Werner, T.; Huber, C.; Wolfbeis, O. S.; Leiner, M. J. P., pH-insensitive ion selective optode: A coextraction-based sensor for potassium ions. *Analytical Chemistry* **1999,** *71* (8), 1544-1548.
58. Du, X.; Xie, X., Non-Equilibrium Diffusion Controlled Ion-Selective Optical Sensor for Blood Potassium Determination. *Acs Sensors* **2017,** *2* (10), 1410-1414.
59. Reisch, A.; Didier, P.; Richert, L.; Oncul, S.; Arntz, Y.; Mély, Y.; Klymchenko, A. S., Collective fluorescence switching of counterion-assembled dyes in polymer nanoparticles. *Nature Communications* **2014,** *5* (1), 4089.
60. Reisch, A.; Trofymchuk, K.; Runser, A.; Fleith, G.; Rawiso, M.; Klymchenko, A. S., Tailoring Fluorescence Brightness and Switching of Nanoparticles through Dye Organization in the Polymer Matrix. *ACS Applied Materials & Interfaces* **2017,** *9* (49), 43030-43042.
61. Würthner, F., Aggregation-Induced Emission (AIE): A Historical Perspective. *Angewandte Chemie International Edition* **2020,** *59* (34), 14192-14196.
62. Laursen, B. V.; Rosenberg, M.; Sorensen, T. J., Azatriangulenium salts as PET-quenched fluorescent probes. Google Patents: 2019.
63. Hargenrader, G. N.; Weerasooriya, R. B.; Ilic, S.; Niklas, J.; Poluektov, O. G.; Glusac, K. D., Photoregeneration of Biomimetic Nicotinamide Adenine Dinucleotide Analogues via a Dye-Sensitized Approach. *ACS Applied Energy Materials* **2018,** *2* (1), 80-91.
64. Guin, J.; Besnard, C.; Pattison, P.; Lacour, J., Highly selective additions of hydride and organolithium nucleophiles to helical carbenium ions. *Chemical Science* **2011,** *2* (3), 425.
65. Kel, O.; Sherin, P.; Mehanna, N.; Laleu, B.; Lacour, J.; Vauthey, E., Excited-state properties of chiral [4]helicene cations. *Photochem. Photobio. Sci.* **2012,** *11* (4), 623-631.
66. Pascal, S.; Besnard, C.; Zinna, F.; Di Bari, L.; Le Guennic, B.; Jacquemin, D.; Lacour, J., Zwitterionic [4]helicene: a water-soluble and reversible pH-triggered ECD/CPL chiroptical switch in the UV and red spectral regions. *Org Biomol Chem* **2016,** *14* (20), 4590-4.
67. Bosson, J.; Gouin, J.; Lacour, J., Cationic triangulenes and helicenes: synthesis, chemical stability, optical properties and extended applications of these unusual dyes. *Chem Soc Rev* **2014,** *43* (8), 2824-40.
68. Ref to NP paper
69. Rosenberg, M.; Junker, A. K. R.; Sørensen, T. J.; Laursen, B. W., Fluorescence pH Probes Based on Photoinduced Electron Transfer Quenching of Long Fluorescence Lifetime Triangulenium Dyes. *ChemPhotoChem* **2019,** *3* (5), 233-242.
70. Mikkelsen, M. B.; Marie, R.; Hansen, J. H.; Wencel, D.; McDonagh, C.; Nielsen, H. O.; Kristensen, A., Controlled deposition of sol–gel sensor material using hemiwicking. *Journal of Micromechanics and Microengineering* **2011,** *21* (11), 115008.
71. Frankær, C. G.; Rosenberg, M.; Santella, M.; Hussain, K. J.; Laursen, B. W.; Sørensen, T. J., Tuning the p K a of a pH Responsive Fluorophore and the Consequences for Calibration of

Optical Sensors Based on a Single Fluorophore but Multiple Receptors. *Acs Sensors* **2019,** *4* (3), 764-773.
72. Sørensen, T. J.; Rosenberg, M.; Frankær, C. G.; Laursen, B. W., An Optical pH Sensor Based on Diazaoxatriangulenium and Isopropyl‐Bridged Diazatriangulenium Covalently Bound in a Composite Sol‐Gel. *Advanced Materials Technologies* **2019,** *4* (2), 1800561.